European Journal of Material Sciences
Vol.4, No.1, pp.1-25, April 2017
Published by European Centre for Research Training and Development UK (www.eajournals.org)

EFFECT OF CALCINATION PROCESS ON CHARACTERIZATION OF THE $Co_{1-x}Zn_xFe_2O_4$ NANOPARTICLES BY CO-PRECIPITATION METHOD

Ahmed Saied Faheim El-Saaey *[1], Abd El Fattah Mustafa Khourshid [2]
Wagih W. Marzouk [3], Samir Mohamed Abdel-Rahman[4]
[1]Mechanical& electrical research institute, National water research Centre, Egypt
[2]Production& Design Department, Faculty of Engineering, Tanta University, Egypt
[3]Production& Design Department, Faculty of Engineering, Minia University, Egypt
[4]Mechanical& electrical research institute, National water research Centre, Egypt

Email: Ahmed Saied Faheim El-Saaey – Egypt_tech2009@yahoo.com
** Corresponding author*

ABSTRACT:*The $Co_{1-x}Zn_xFe_2O_4$ Nanoparticles ($Co_{1-x}Zn_xFe_2O_4$. with x = 0.0, 0.1, 0.3, 0.5, 0.7, 0.9 and 1, With exposure to a calcination temperature of 100, 300, 600 and 900 °C) synthesized by the Co-precipitation method .The structural and magnetic properties of the products were determined and characterized in detail by X-ray diffraction (XRD), High Resolution -Transmission Electron Microscope (HR-TEM), Energy Dispersive X-ray Spectroscopy (EDX) , Fourier Transform Infrared (FTIR) and vibrating sample magnetometer (VSM). These results provided that all the samples prepared at the nano-scale. X-ray analysis showed that the samples were cubic spinel structural (kind of inverse spinel oxide).The crystallinity is improved with the increases calcination temperature for all samples and that proved by the FT-IR , XRD and EDX results and compound purity fabricated. HR-TEM analysis showed that nanoparticles size and the shape based on the Zn concentration & the calcination temperatures and also indicates that degree of agglomeration for all samples. VSM analysis showed that The C4 ($Co_{0.5}Zn_{0.5}Fe_2O_4$ at 600°C) is best sample in Magnetic &structure properties where it's super-paramagnetic behavior.*

KEYWORDS: Calcination process; Co-precipitation method; $Co_{0.3}Zn_{0.7}Fe_2O_4$ Nanoparticles; Ferrite; Magnetic properties.

INTRODUCTION

Ferrite (MFe_2O_4) is one of the most important types of ceramic materials, which played an important role in many of the modern industrial processes, for example Radar-absorbent material, remove the oil from the water, drug delivery system, Electric Transformers and motor industry for being possesses high magnetic and electrical properties ,As well as the electronics industry and Paints. Cobalt zinc ferrite ($Co_{1-x}Zn_xFe_2O_4$) is an inverse spinel structure where $[Zn_x^{2+}Fe_{(1-x)}^{3+}]_A$

Print ISSN: ISSN 2055-8112(Print); Online ISSN: ISSN 2055-8120(Online)

ions are occupied at "A" site (tetrahedral site) and $[Co^{2+}_{(1-x)}Fe^{3+}_{(1+x)}]_B$ ions are accommodated at "B" site (octahedral site). The $Co_{1-x}Zn_xFe_2O_4$ Nanoparticles are fabricated by many techniques such as sol–gel, combustion methods, wet high energy ball milling, hydrothermal, electrochemical, refluxing, solvothermal and co-precipitation method [1:19]. With the diversity of techniques produced the co-precipitation method Characterized from the other methods as an economical, environment-friendly and does not require any complex technologies. The aim of the present work is to the synthesis of $Co_{1-x}Zn_xFe_2O_4$ Nanoparticles by Co-precipitation method within calcination process at four different temperatures namely 100 °C, 300°C, 600°C and 900°C with its effect study on characteristic of $Co_{1-x}Zn_xFe_2O_4$ Nanoparticles. The synthesized Nano- crystals have been characterized by XRD, HR-TEM, EDX, vibrating sample magnetometer (VSM) and FT-IR, provided below are the investigation details.

MATERIALS AND METHODS:

It was the $Co_{1-x}Zn_xFe_2O_4$ Nanoparticles are fabricated by co-precipitation method using the following chemicals; $CoCl_2.6H_2O$, $ZnCl_2$ and $FeCl_3.6H_2O$ are produced by the SD fine-CHEM Limited Co., addition to sodium hydroxide is produced by EL-Naser Pharmaceutical chemical Co., were purchased from (El-Gomhouria Co. for Drugs) , Egypt and used as received without further treatment.

Manufacturing steps description of the $Co_{1-x}Zn_xFe_2O_4$ Nanoparticles ($Co_{1-x}Zn_xFe_2O_4$. with x = 0.0, 0.1, 0.3, 0.5, 0.7, 0.9 and 1, the defined from 1: 7 respectively, With exposure to a calcination temperature of 100, 300, 600 and 900 °C, the defined from A,B,C and D respectively) is shown in Figure (2.1).

Characterization Techniques:

X-ray powder diffraction analysis was conducted on a Brucker Axs-D8 Advace Diffractometer (XRD). FTIR transmission spectra were taken on Perkin Elmer Spectrum BX model Infrared Spectrophotometer from 2000 to 400 cm^{-1}.High Resolution- Transmission Electron Microscopy (HR-TEM) analysis was performed on (JEOL 2000FX). Magnetic measurements were carried out with the Quantum Design Model 6000 Vibrating Sample Magnetometer (VSM) and parameters like specific saturation magnetization (Ms), coercive force (H_c) and remanence (Mr) were evaluated.

Print ISSN: ISSN 2055-8112(Print); Online ISSN: ISSN 2055-8120(Online)

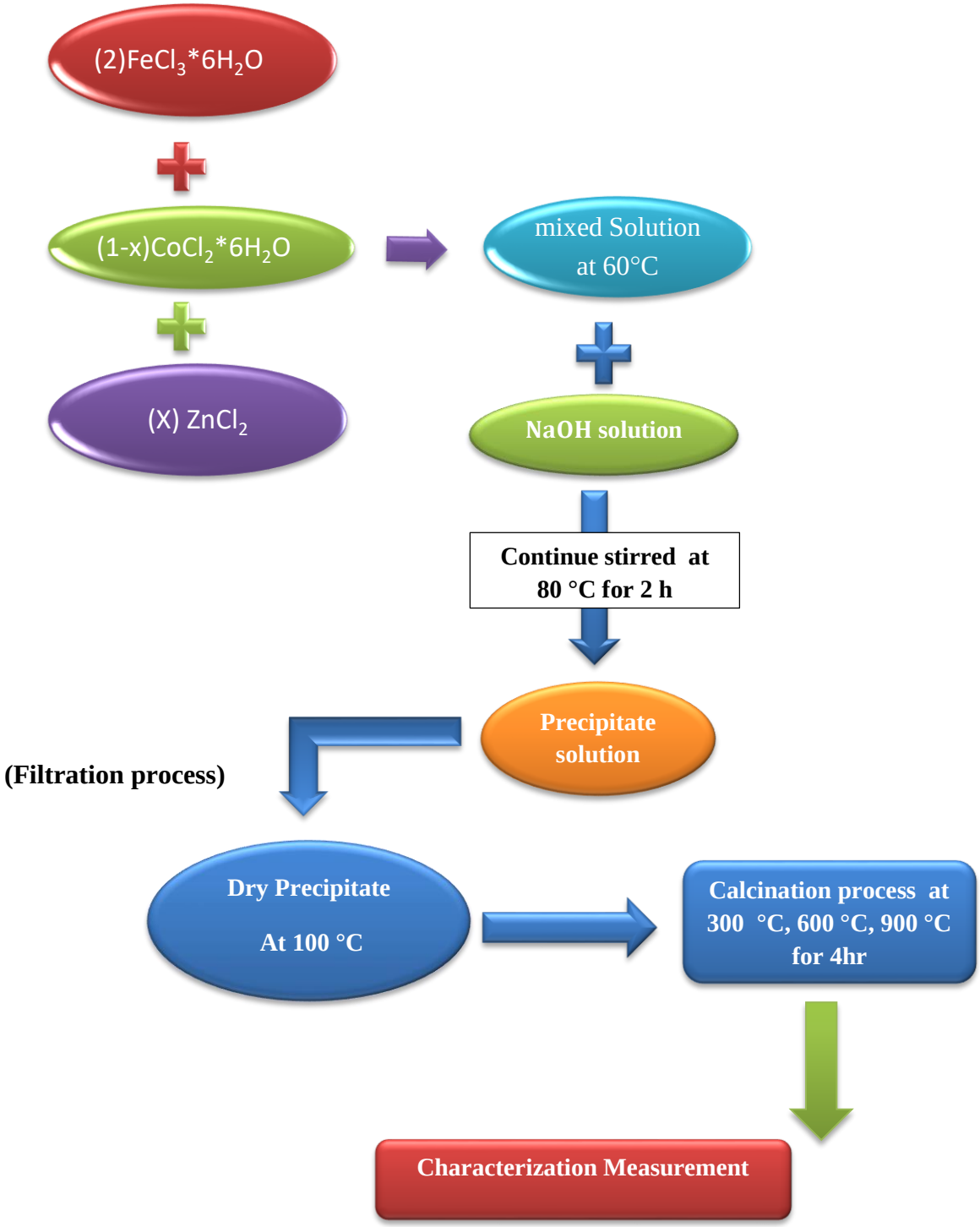

Figure 2.1. Flow chart showing the fabrication of the $Co_{1-x}Zn_xFe_2O_4$ Nanoparticles

Print ISSN: ISSN 2055-8112(Print); Online ISSN: ISSN 2055-8120(Online)

RESULTS AND DISCUSSION

3.1 Structural properties

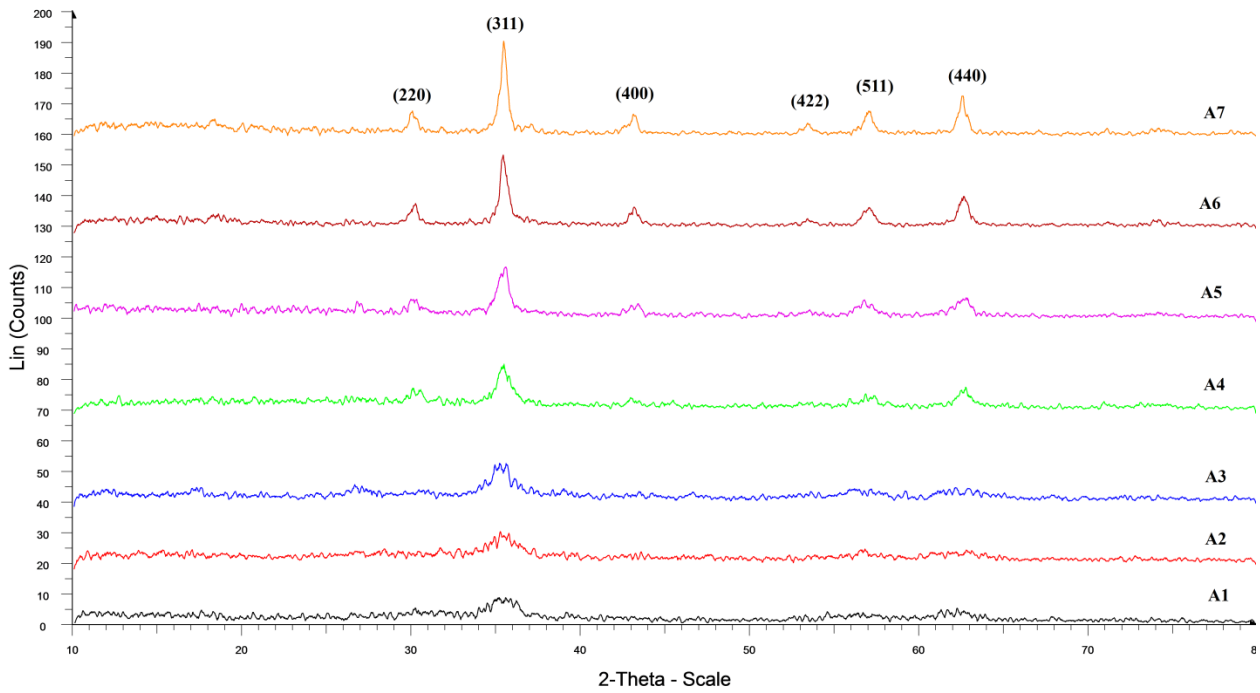

Figure (3.1) : the X-ray diffraction patterns of $Co_{1-x}Zn_xFe_2O_4$ nanoparticles at 100 °C

Print ISSN: ISSN 2055-8112(Print); Online ISSN: ISSN 2055-8120(Online)

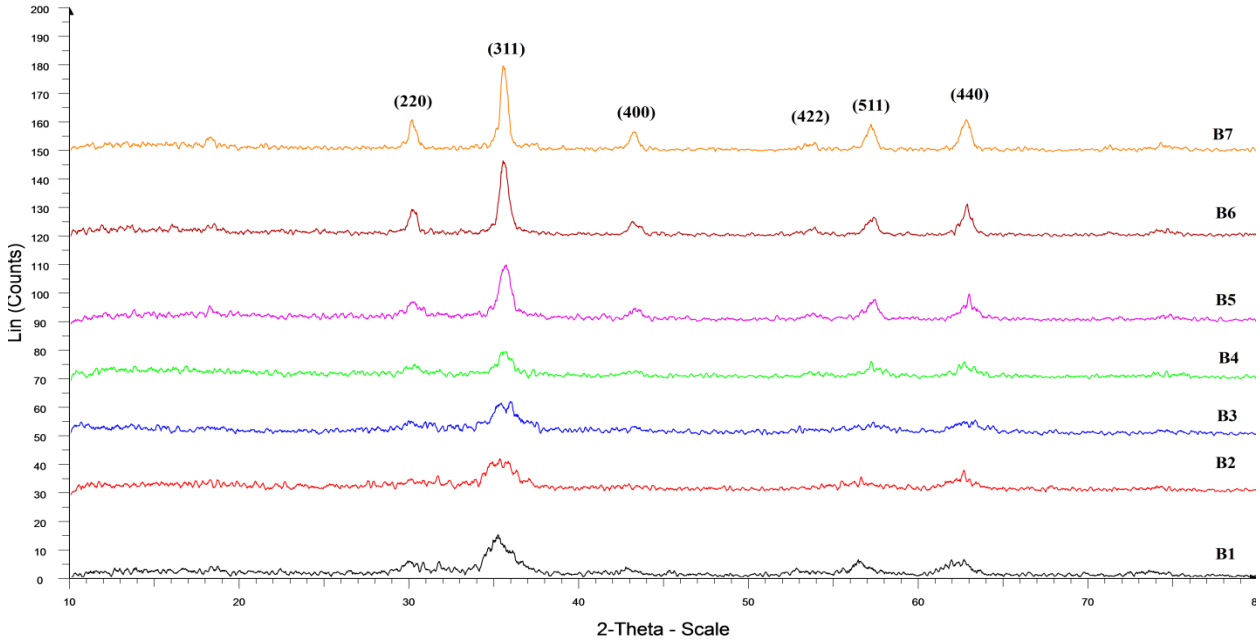

Figure (3.2) : the X-ray diffraction patterns of $Co_{1-x}Zn_xFe_2O_4$ nanoparticles at 300 °C

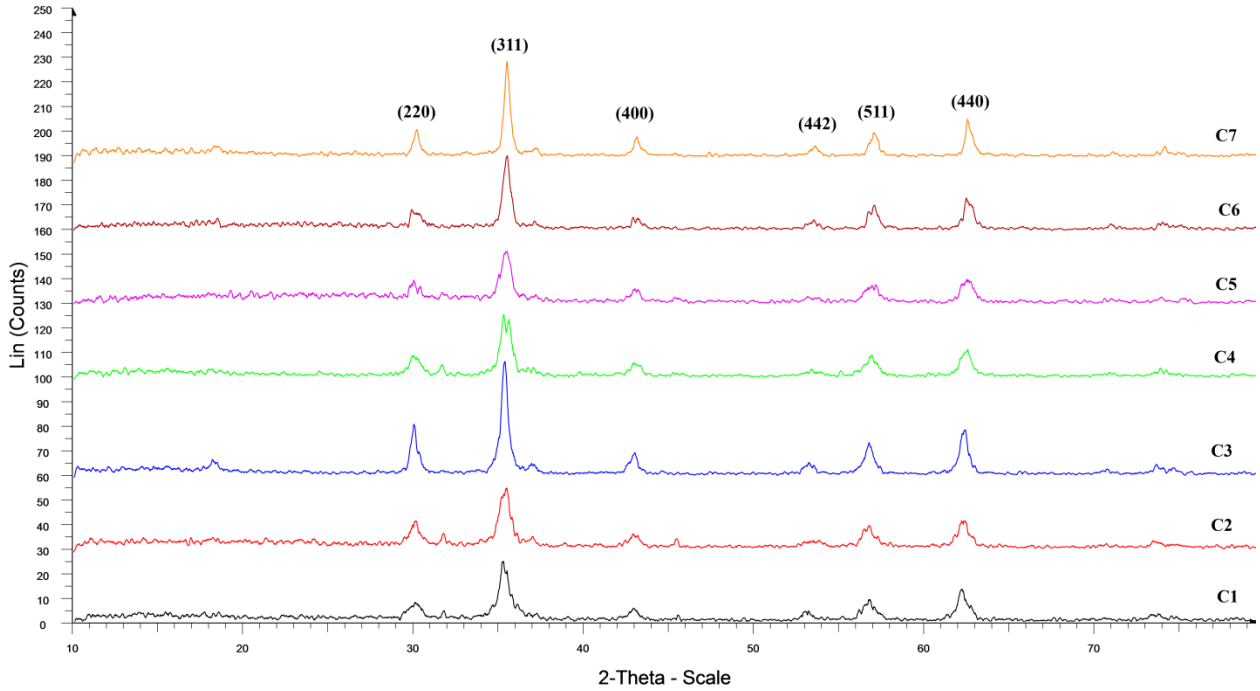

Figure (3.3) : the X-ray diffraction patterns of $Co_{1-x}Zn_xFe_2O_4$ nanoparticles at 600°C

Print ISSN: ISSN 2055-8112(Print); Online ISSN: ISSN 2055-8120(Online)

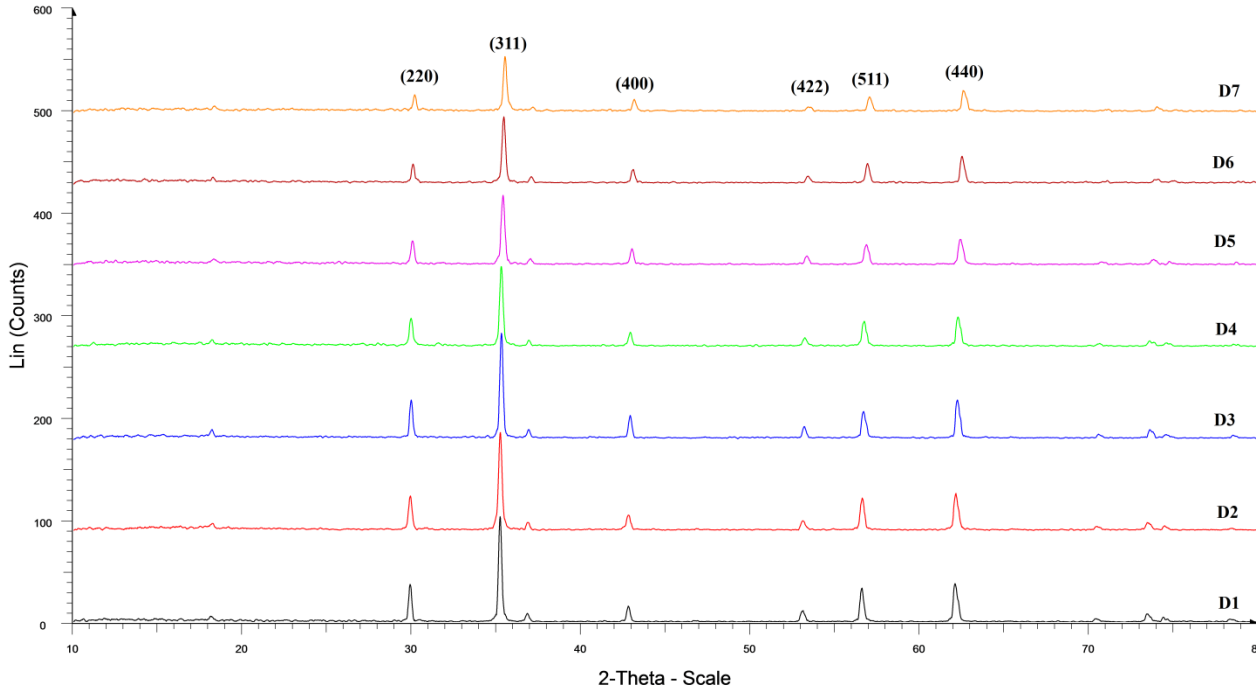

Figure (3.4) : the X-ray diffraction patterns of $Co_{1-x}Zn_xFe_2O_4$ nanoparticles at 900 °C

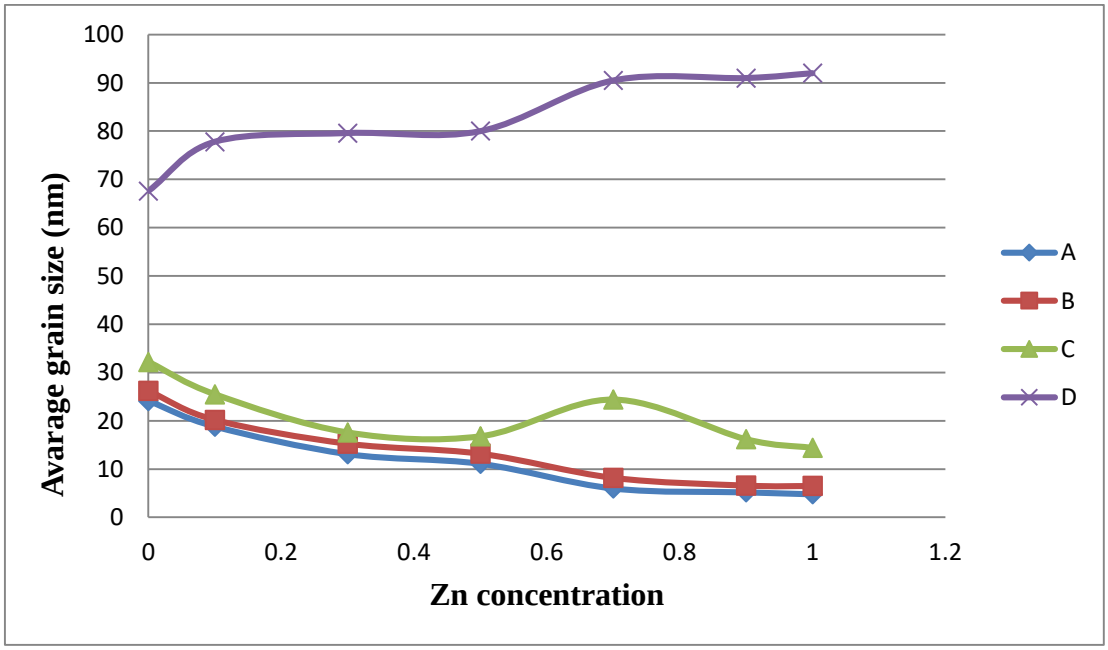

Figure(3.5): the average grain size of $Co_{1-x}Zn_xFe_2O_4$ nanoparticles samples calcined at difference temperature

Print ISSN: ISSN 2055-8112(Print); Online ISSN: ISSN 2055-8120(Online)

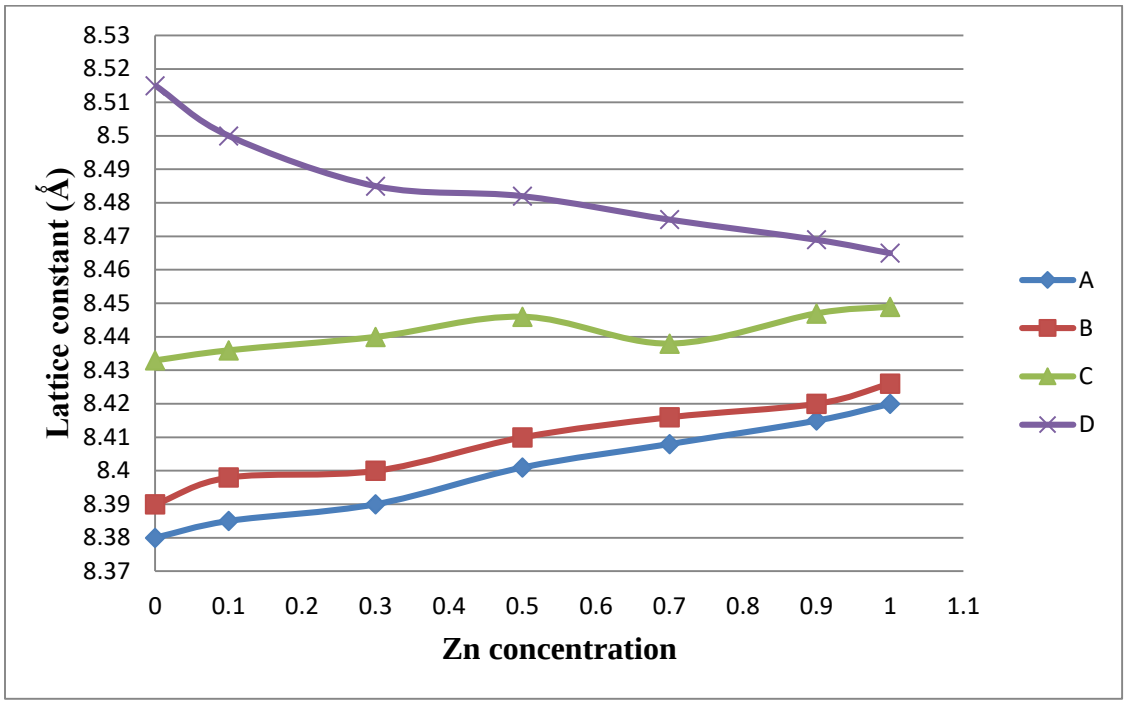

Figure (3.6): the lattice constsnt of $Co_{1-x}Zn_xFe_2O_4$ nanoparticles samples calcined at difference temperature

In figures (3.1:3.4) show the X-ray diffraction patterns of $Co_{1-x}Zn_xFe_2O_4$ nanoparticles samples at different temperatures. The diffraction patterns show six reflection planes (220), (311), (400), (422), (511), (440) without impurities reflection [20 ,21]. These clear-cut musings without any confusion, exhibits the formation of a spinel cubic structure and the (hkl) value of the entire peak are which refer to face centered cubic (F.C.C.) structure (kind of inverse spinel oxide).The broad x-ray diffraction peak for the samples calcined at 600°C suggest that the $Co_{1-x}Zn_xFe_2O_4$ particles are of nano size, whereas calcination achieve about increase in grain size which leads rise to sharp clear-cut peaks due to more crystalline (degree of crystallinity) from A &B samples groups (at 100 ºC and 300 ºC), so the sharper and narrower peak as compared to A & B samples at 100 ºC and 300 ºC, this is obvious in the figures(1,2,3). The sharpness of the XRD pattern shows that degree of crystallinity is increased with increasing the calcination temperature; however the peak of the XRD spectra of $Co_{1-x}Zn_xFe_2O_4$ nanoparticles calcined at 900 ºC. Figure (4), shows that peaks is sharper at this temperature as compared to the previous peaks [22]. The XRD analysis, the average grain size for each sample has been calculated from the XRD line width of the highest intensity peak (311) using Debye Scherrer equation and the lattice parameter a_o can be calculated using the relation $a_o = d\,(h^2 + k^2 + L^2)^{1/2}$ [23,24].

Print ISSN: ISSN 2055-8112(Print); Online ISSN: ISSN 2055-8120(Online)

In figure (3.5) shows that the average grain size of $Co_{1-x}Zn_xFe_2O_4$ nanoparticles at 100 ºC, 300 ºC, 600 ºC and **900°C** is **increased with increasing calcination temperatures from 100 °C to 900°C and its decreased with increasing Zn concentration** at 100 ºC, 300 ºC, 600 ºC and inverse trend with 900 ºC. This increase the average grain size due to increasing degree of crystallinity. In figure (3.6) shows that the lattice constant of $Co_{1-x}Zn_xFe_2O_4$ nanoparticles at 100 ºC, 300 ºC, 600 ºC and **900°C** is **increased with increasing calcination temperatures from 100 °C to 900°C and its increased with increasing Zn concentration** at 100 ºC, 300 ºC, 600 ºC and inverse trend with 900 ºC, this **increase lattice constant because difference in ionic radii of** Zn^{2+} **and** Co^{2+} and Zn^{2+}**will cause migration of** Fe^{3+} **from A−site to B−site [25,** 26, 27 **].**

FTIR studies

Figures (3.7:3.10) gives the infrared spectra of the investigated $Co_{1-x}Zn_xFe_2O_4$(x = 0.0: 1.0), from which it can be seen that there are two bands characterizing ferrites. The values of absorption band position depend on the cation distribution of compositions. The difference in position of the bands for the various compositions is expected due to the difference in the stretching of bonds between octahedral or tetrahedral metal ions and oxide ions (bond length).[28]

The FTIR absorption bands for two techniques at room temperature in the wave number range of 400–2000 cm^{-1}It is clear that the higher frequency band is (υ_1) around ≈ 600 $cm^{-1}$and the lower frequency band (υ_2) is around ≈ 400 cm^{-1}. It is observed that (υ_1) band linearly increases with the increase in Zn^{2+}ion content and calcination temperature while (υ_2) band do not vary much. As Zn^{2+} ions entirely occupy mostly the tetrahedral sites and force Fe^{3+}, Co^{2+} ions to occupy octahedral sites with the increase in Zn ions. There fore the radius of the tetrahedron becomes larger and that of octahedral hardly change with Zn content and calcination temperature [29,30]. Generally the presence of the bands characteristics for $Co_{1-x}Zn_xFe_2O_4$ indicates the formation of ferrite Nanoparticles at all compositions. Therefore, the FT-IR results proved the XRD results that appear the cations distribution, crystal structure phase and degree of crystallinity.

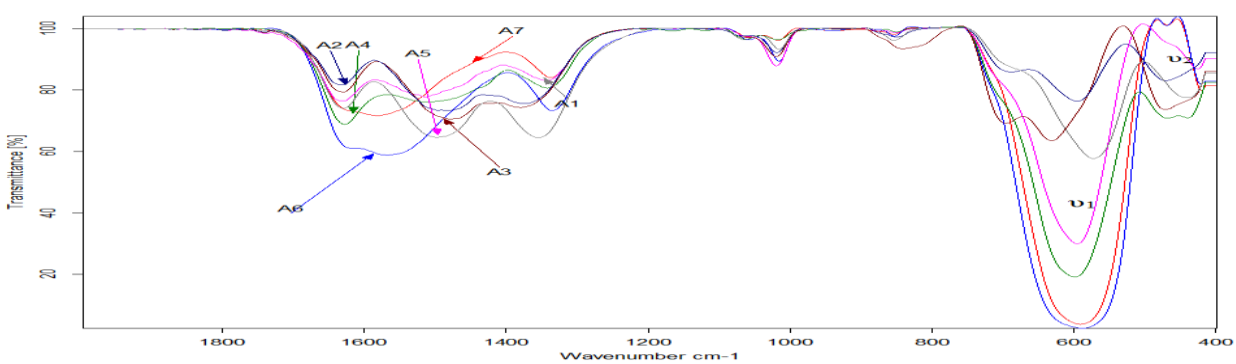

Figure (3.7): The infrared spectra of $Co_{1-x}Zn_xFe_2O_4$ Nanoparticles at 100 °C

Print ISSN: ISSN 2055-8112(Print); Online ISSN: ISSN 2055-8120(Online)

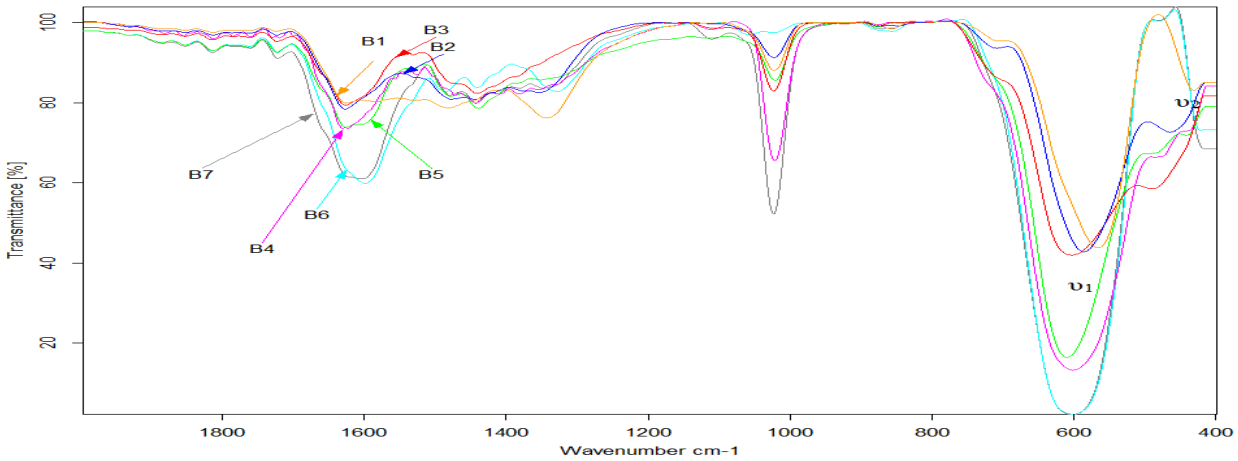

Figure (3.8): The infrared spectra of $Co_{1-x}Zn_xFe_2O_4$ Nanoparticles at 300 °C

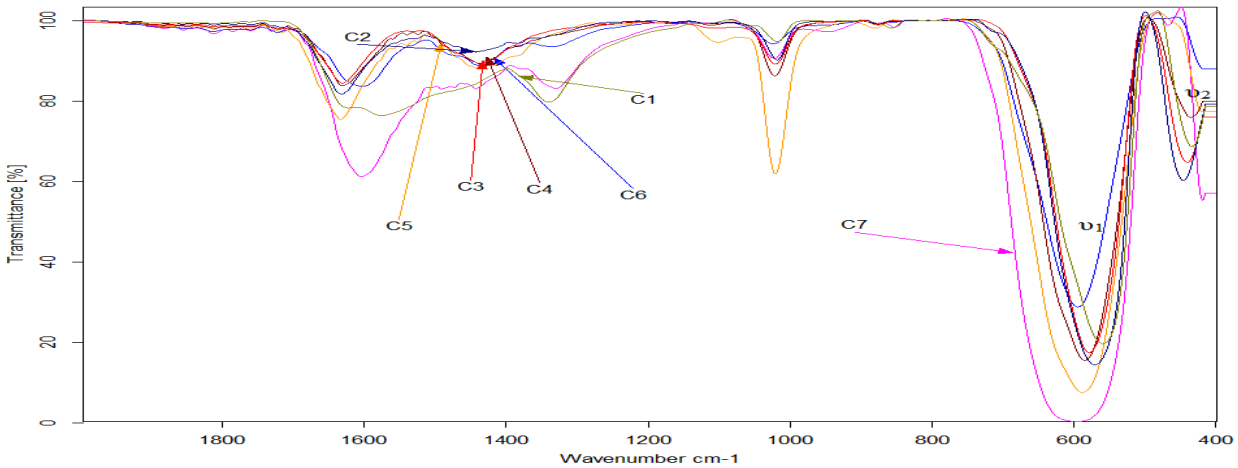

Figure (3.9): The infrared spectra of $Co_{1-x}Zn_xFe_2O_4$ Nanoparticles at 600 °C

Print ISSN: ISSN 2055-8112(Print); Online ISSN: ISSN 2055-8120(Online)

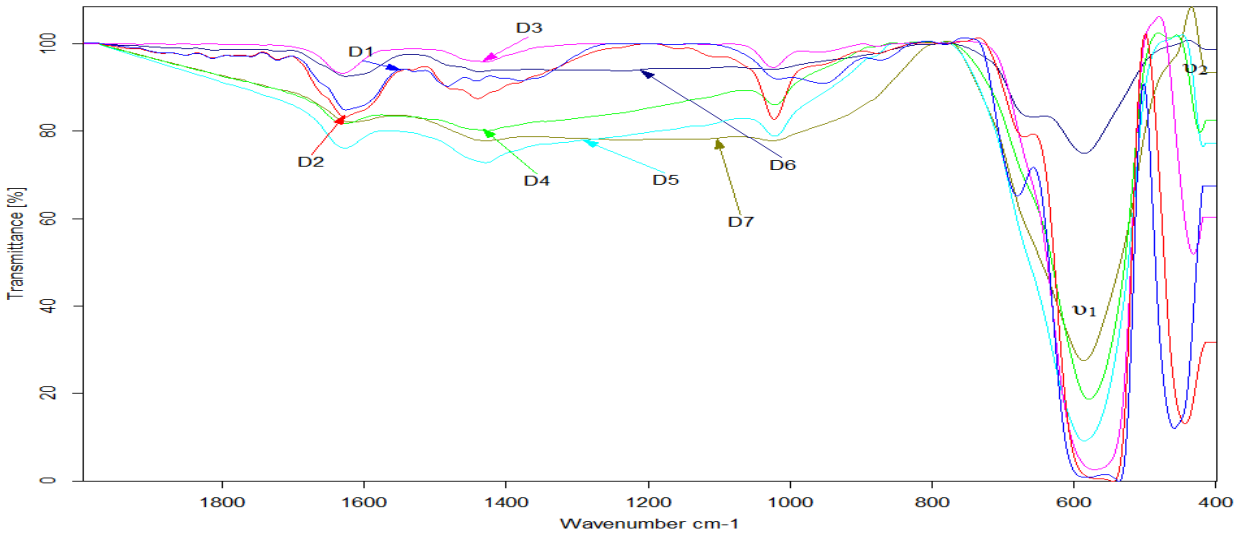

Figure (3.10): The infrared spectra of $Co_{1-x}Zn_xFe_2O_4$ Nanoparticles at 900 °C

The HR- TEM with EDAX (Energy Dispersive X-ray Spectroscopy):

Table (1): The HR- TEM images, The EDX spectrum and quantitative results

Sample	*TEM images*	*The EDX spectrum and quantitative results*
A1	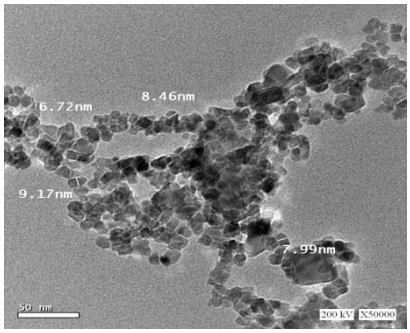	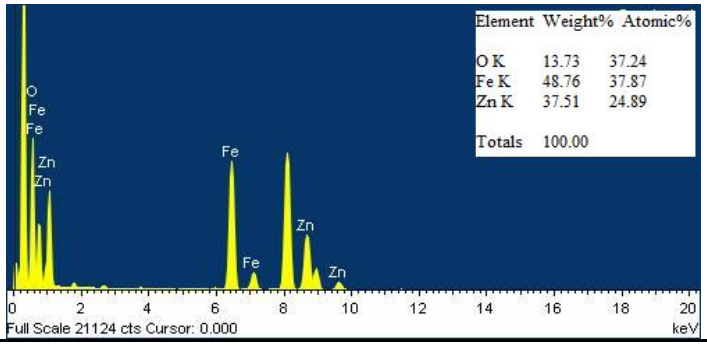
A2	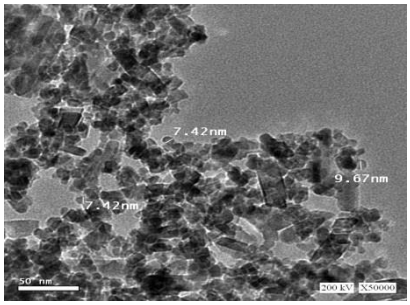	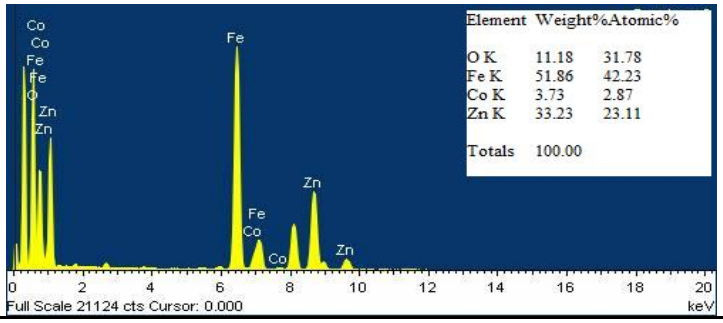

Print ISSN: ISSN 2055-8112(Print); Online ISSN: ISSN 2055-8120(Online)

A3	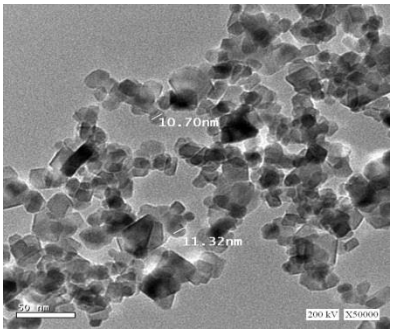	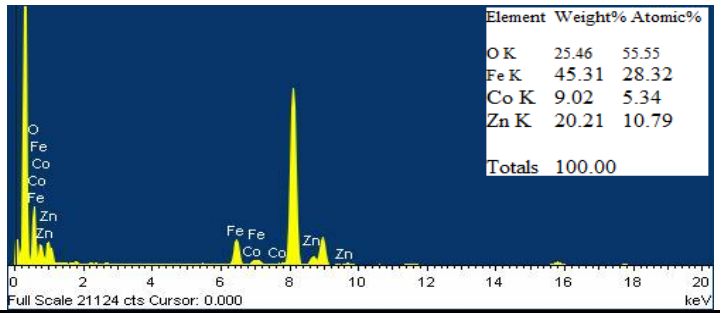
A4	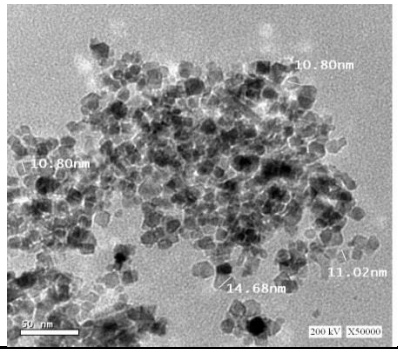	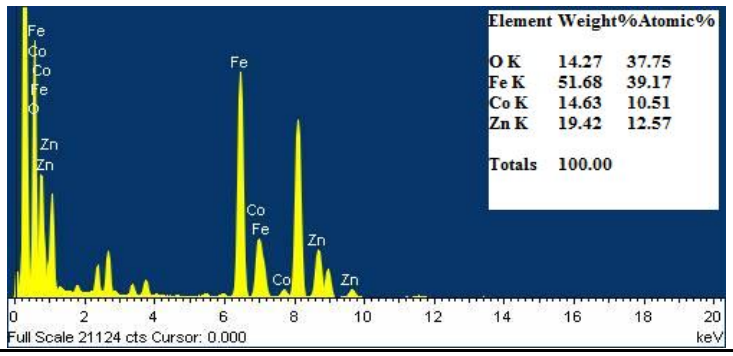
A5	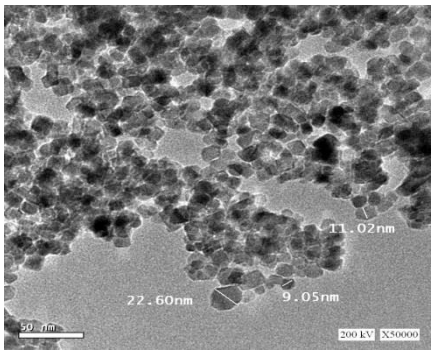	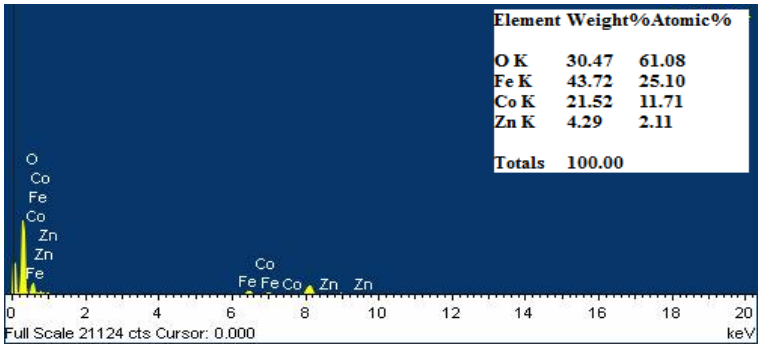
A6	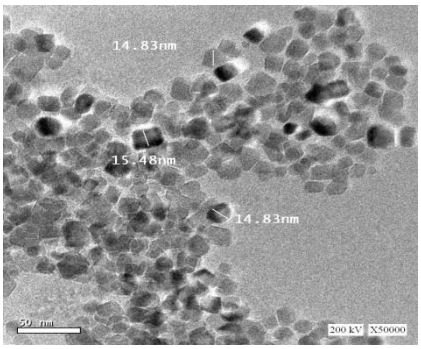	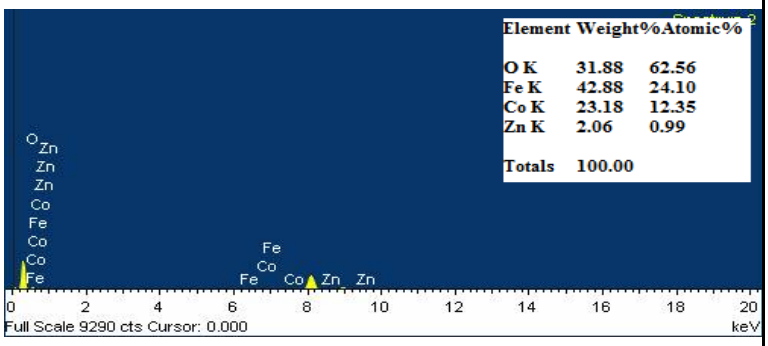

Print ISSN: ISSN 2055-8112(Print); Online ISSN: ISSN 2055-8120(Online)

A7	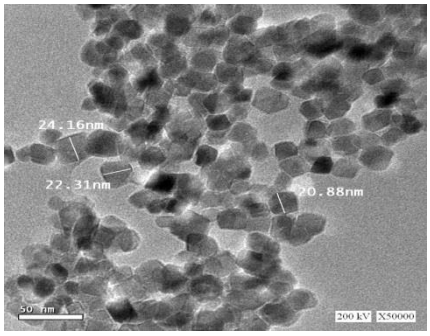	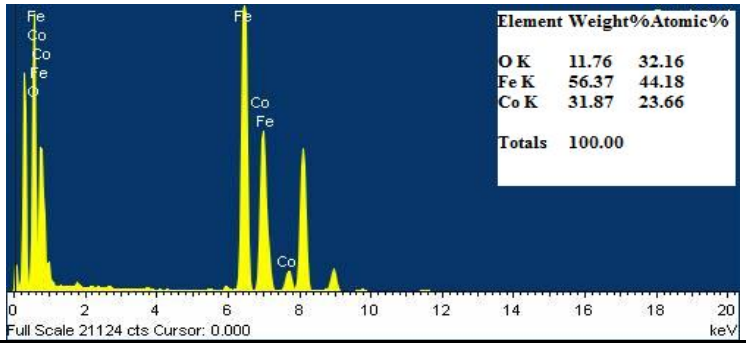
B1	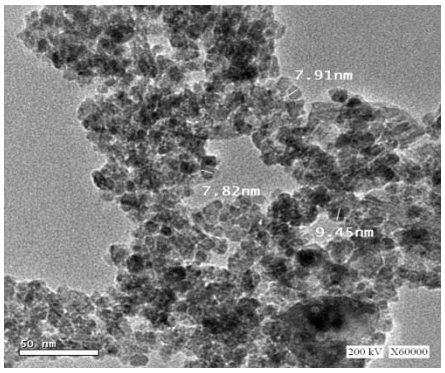	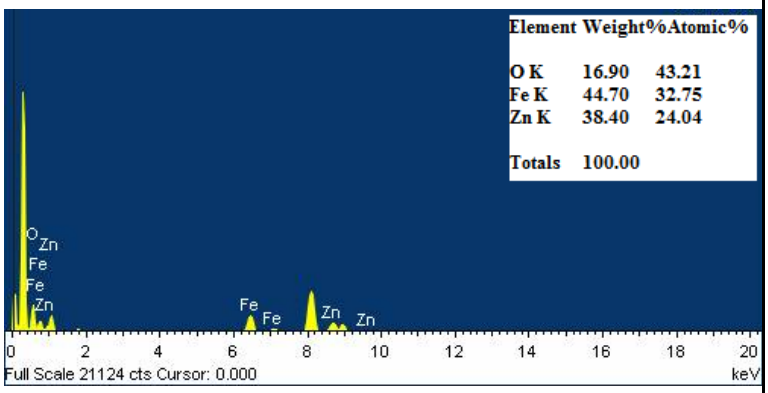
B2	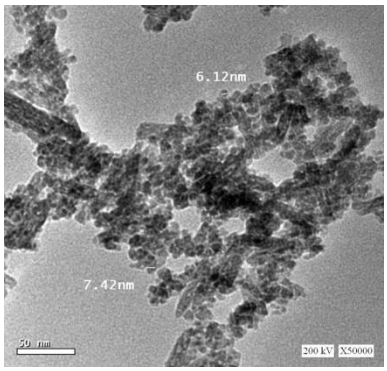	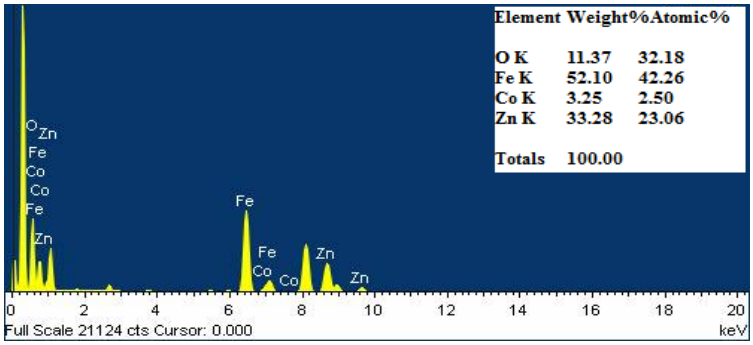
B3	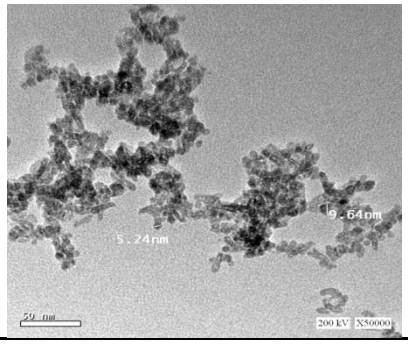	

Print ISSN: ISSN 2055-8112(Print); Online ISSN: ISSN 2055-8120(Online)

		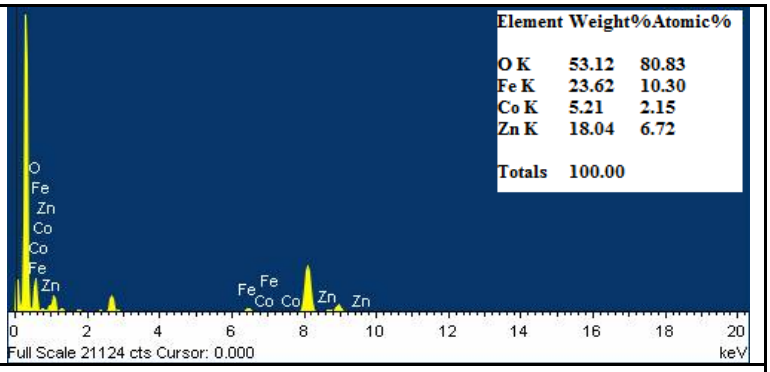
B4	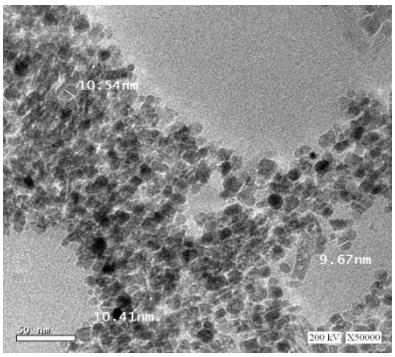	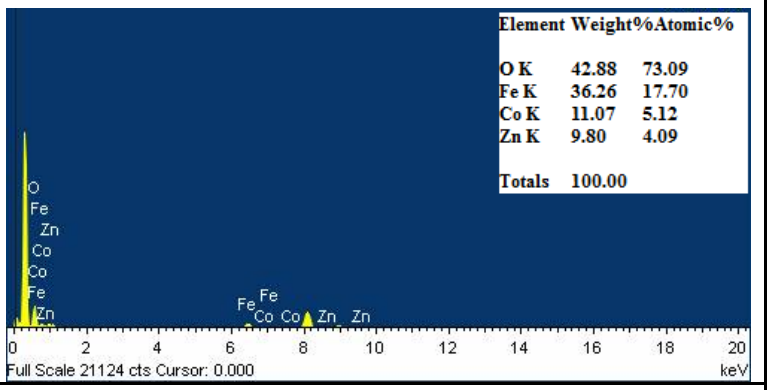
B5	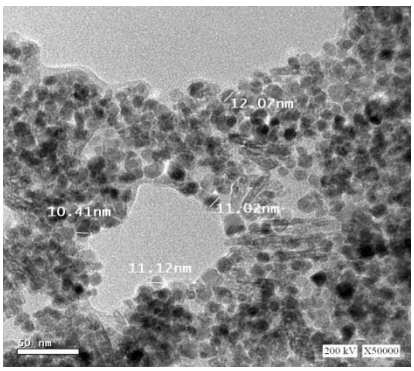	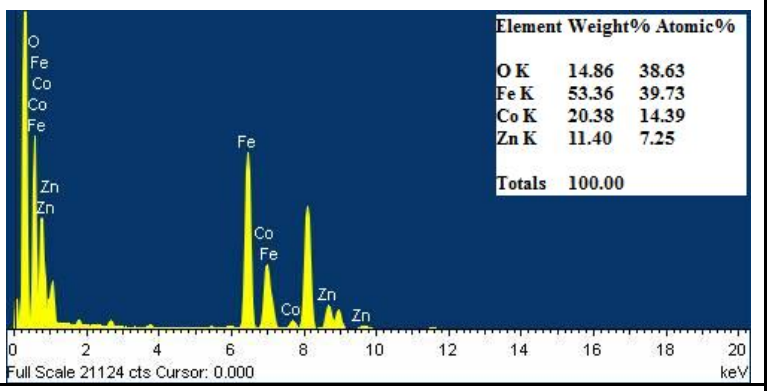
B6	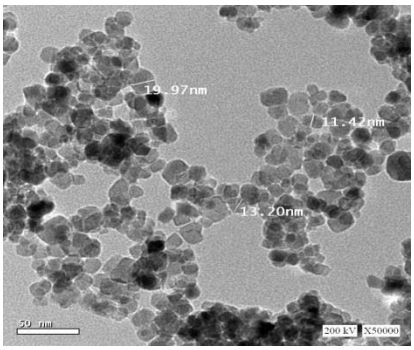	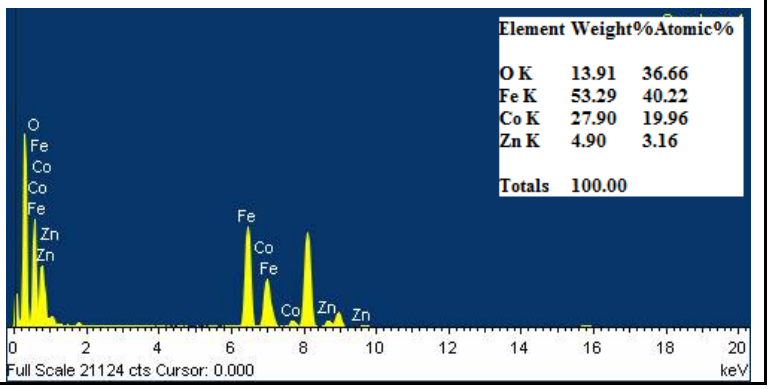

Print ISSN: ISSN 2055-8112(Print); Online ISSN: ISSN 2055-8120(Online)

B7	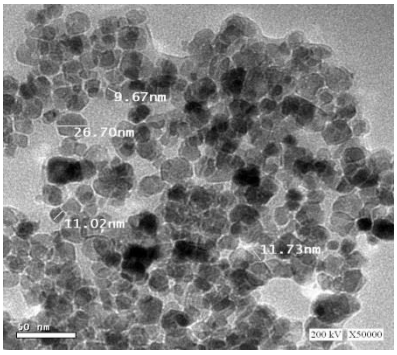	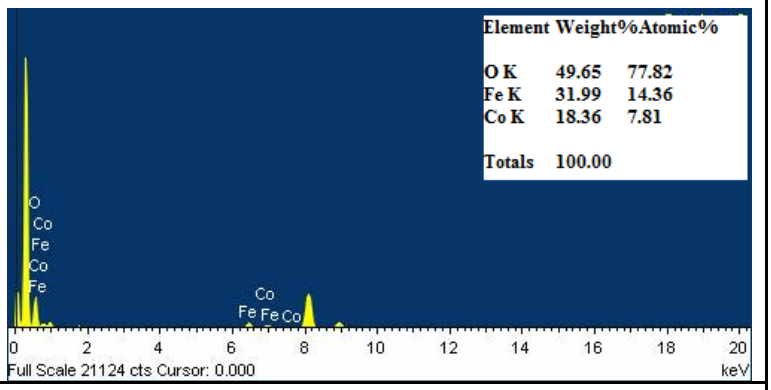
C1	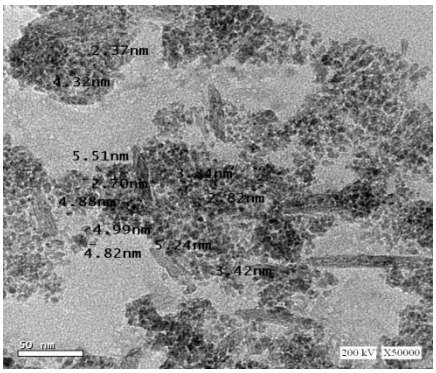	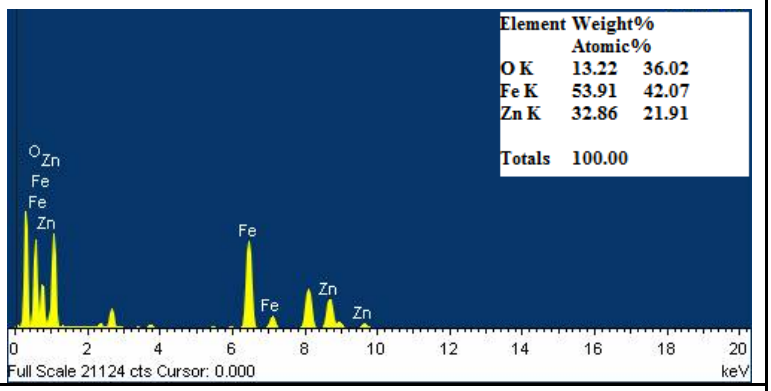
C2	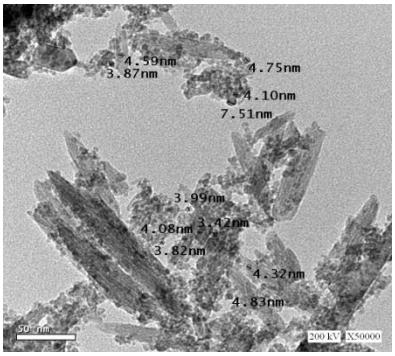	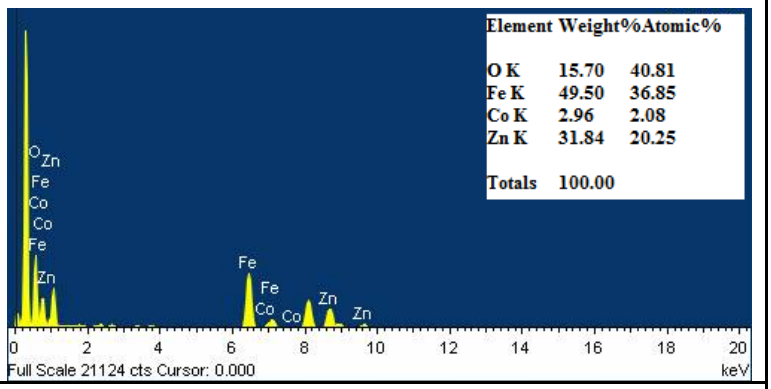
C3	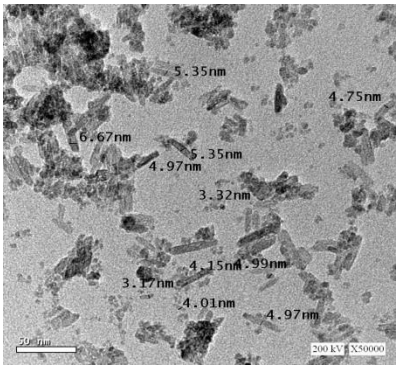	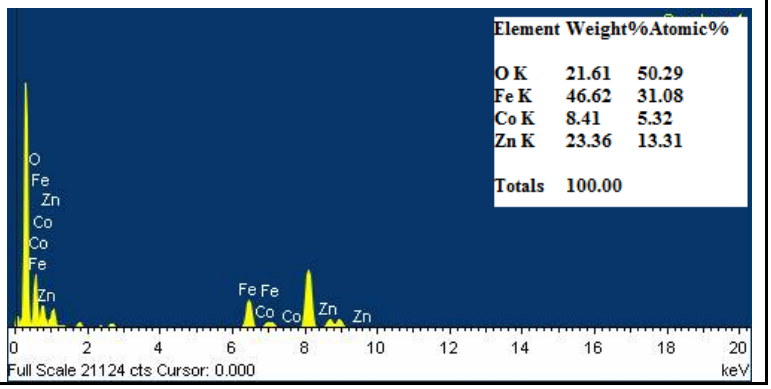

Print ISSN: ISSN 2055-8112(Print); Online ISSN: ISSN 2055-8120(Online)

C4	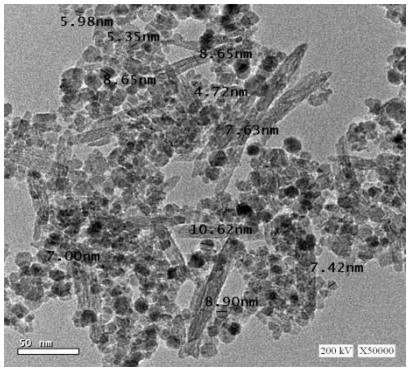	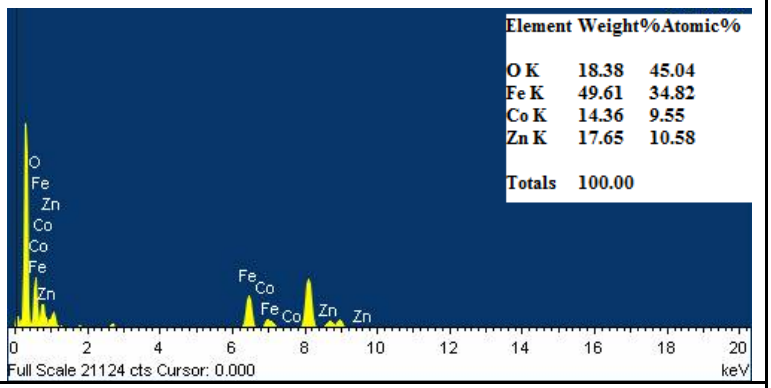
C5	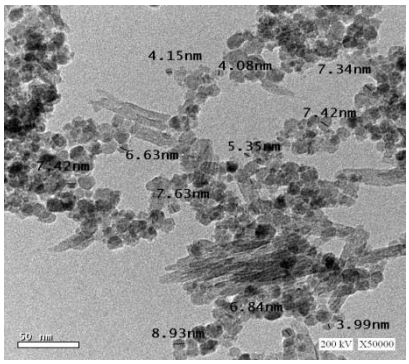	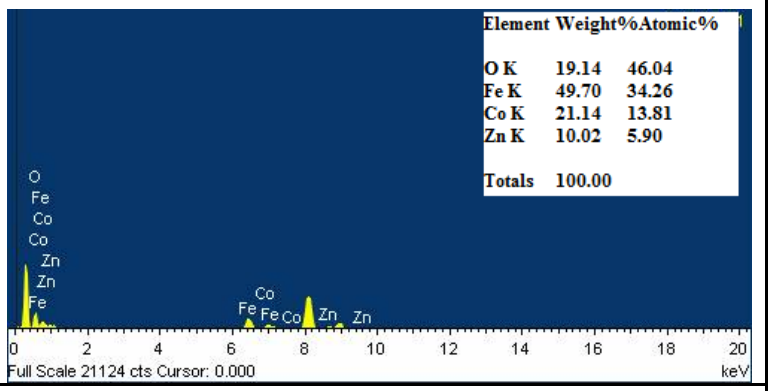
C6	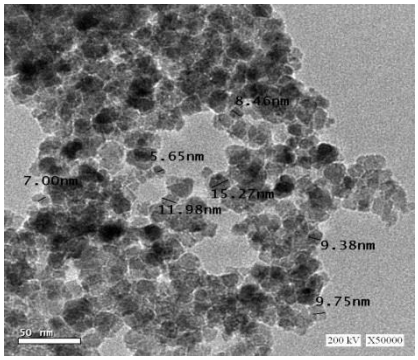	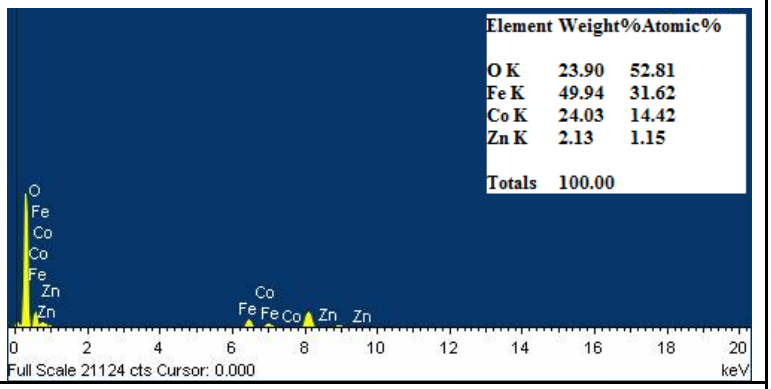
C7	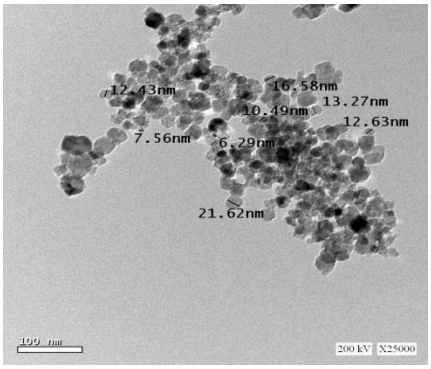	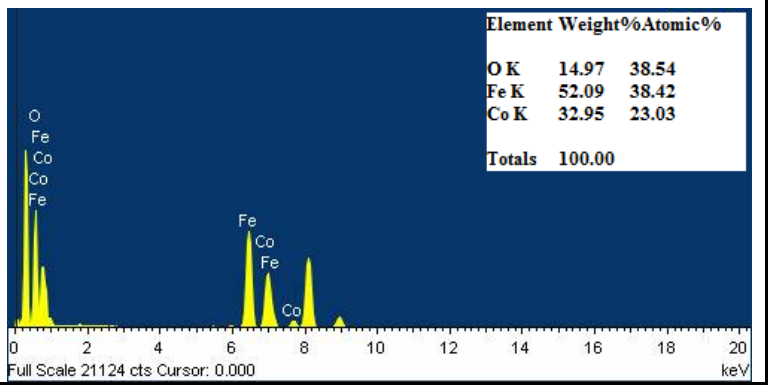

Print ISSN: ISSN 2055-8112(Print); Online ISSN: ISSN 2055-8120(Online)

D1

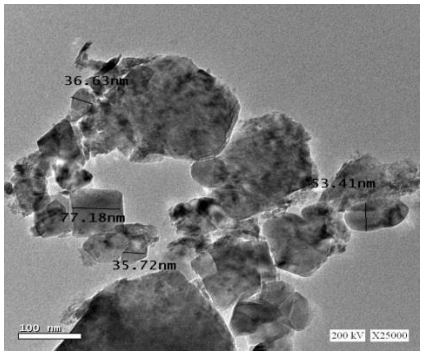

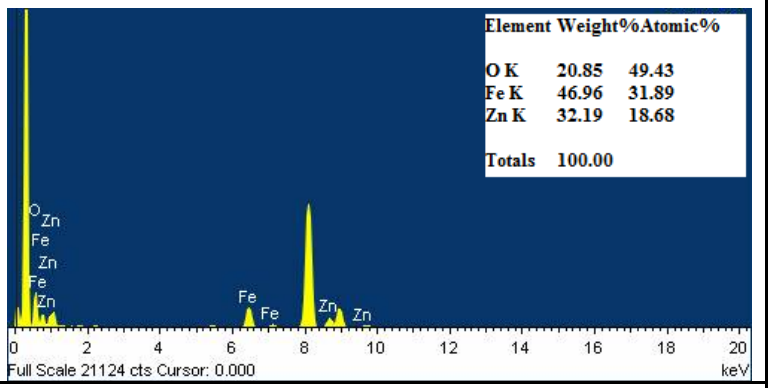

D2

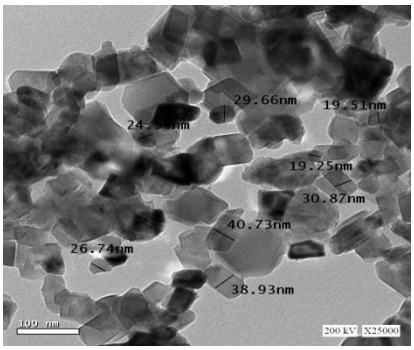

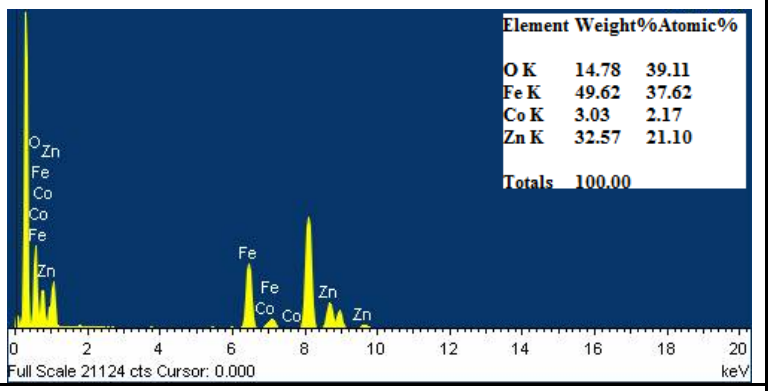

D3

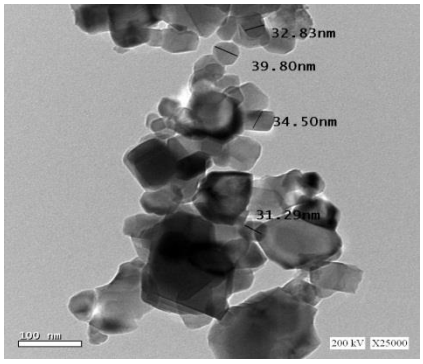

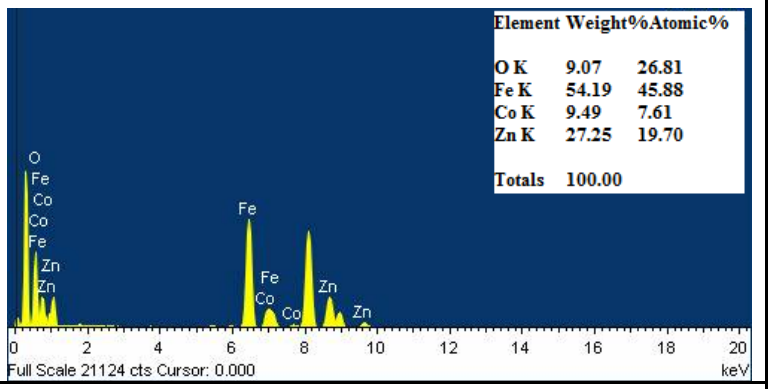

D4

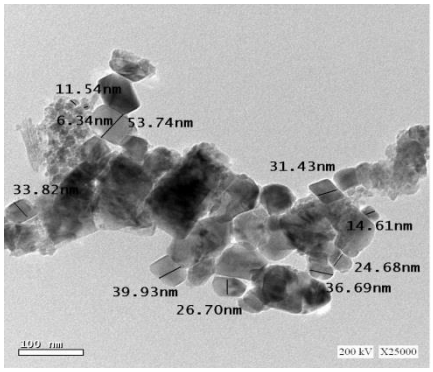

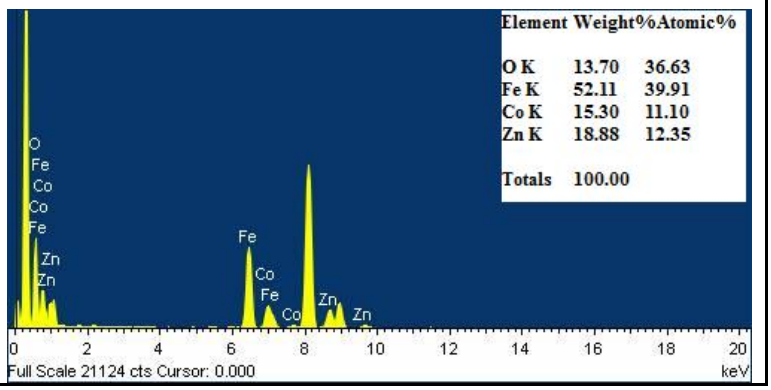

Print ISSN: ISSN 2055-8112(Print); Online ISSN: ISSN 2055-8120(Online)

D5	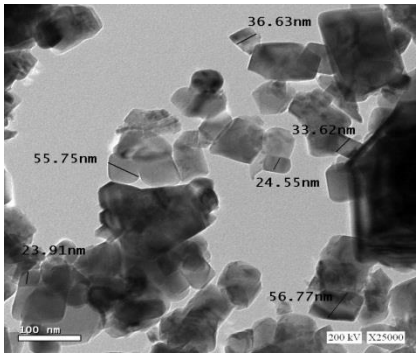	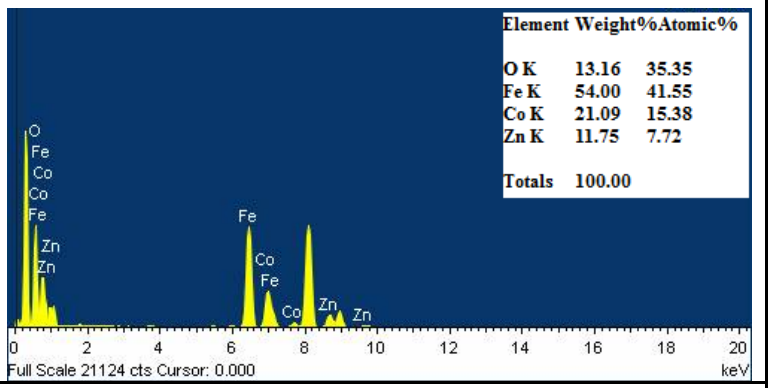
D6	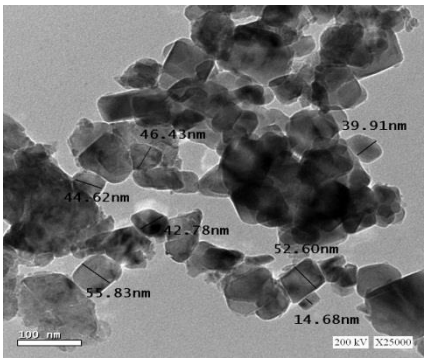	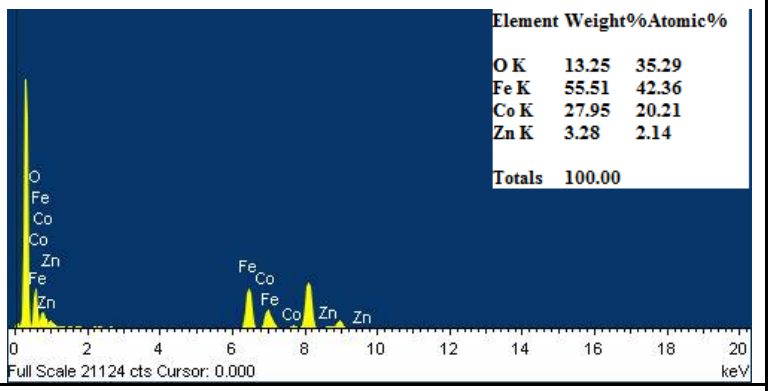
D7	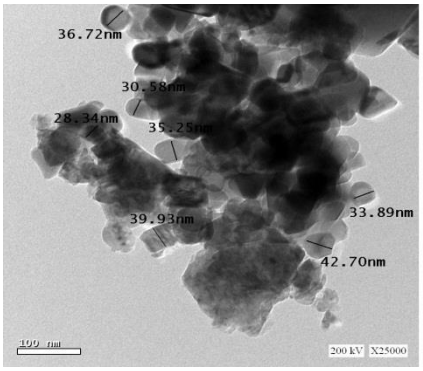	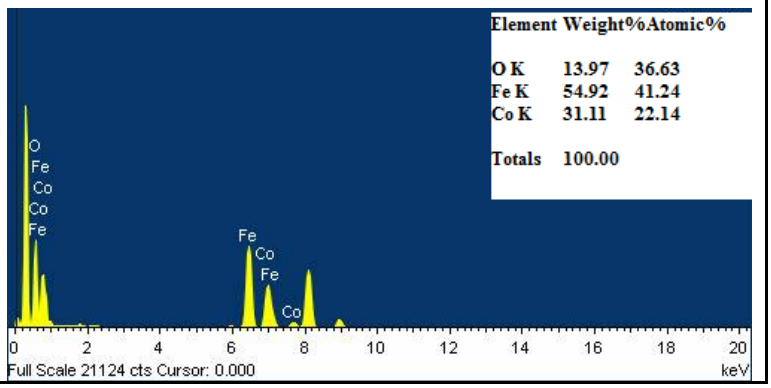

The EDX spectrum and quantitative results of $Co_{1-x}Zn_xFe_2O_4$ at different temperatures are shown in Table (1). From EDX spectrum, the presence of Zn, Fe and O are observed with atomic percentages for $Co_{1-x}Zn_xFe_2O_4$ nanoparticles at different temperatures in Table (1). The EDX analysis showed the absence of any impurities in $Co_{1-x}Zn_xFe_2O_4$ nanoparticles at different temperatures. Therefore, the EDX spectrum results proved the XRD results.

The Nano-Structure of the Cobalt Zinc Ferrite nanoparticles fabricated by Co-precipitation method with change in Zn concentration & calcination parameter (at 100 °C, 300°C,600°C and 900°C),

Print ISSN: ISSN 2055-8112(Print); Online ISSN: ISSN 2055-8120(Online)

are investigated by HR-TEM. The table (1) shows images of the $Co_{1-x}Zn_xFe_2O_4$ nanoparticles at different temperature, these images clear ones that the $Co_{1-x}Zn_xFe_2O_4$ nanoparticles at 100 °C and 300°C take the spherical form with uniform size, but the calcination temperature increase for $Co_{1-x}Zn_xFe_2O_4$ nanoparticles at 600°C occur change in shapes (spherical and Whiskers combination form) with Zn concentration increase but TEM images at B6 & B7 are spherical form only. The images of $Co_{1-x}Zn_xFe_2O_4$ nanoparticles at 900°C take the spherical form only with uniform size. Therefore, the HR-TEM results proved the XRD results that appear the nanoparticle size (grain size) is dependent on the Zn concentration and calcination temperature.

It is shown that the $Co_{1-x}Zn_xFe_2O_4$ nanoparticles at 100 °C and 300°C has a high degree of agglomeration, but the $Co_{1-x}Zn_xFe_2O_4$ nanoparticles at 600 °C and 900°C has a low degree of agglomeration caused by mutual interaction between particles which arises from some parameters such as Vander-walls forces, capillary forces and electrostatic forces[31].

In general, the $Co_{1-x}Zn_xFe_2O_4$ nanoparticles at 100 °C, 300°C and 600°C the agglomeration increase with Zn concentration increase, but it's inverse in the $Co_{1-x}Zn_xFe_2O_4$ nanoparticles at 900 °C .

Magnetic properties:

Figure (3.11) shows the hysteresis loop of the $Co_{1-x}Zn_xFe_2O_4$ nanoparticles at different temperatures. A figure (3.12: 3.15) lists different parameters such as saturation magnetization (Ms), remanent magnetization (Mr), the ratio of remanent magnetization to saturation magnetization (Mr/Ms) and coercivity.

The saturation magnetization of the $Co_{1-x}Zn_xFe_2O_4$ nanoparticles at different temperatures is shown in Figure 3.12 where show that the saturation magnetization increase with Zn concentration decrease. This may due to Zn^{2+} (with zero magnetic moment) replace ion on the tetrahedral A–sites, causing the decrease of magnetic moment in the sublattice M_A, resulting in the increase of total magnetic moment according to Neel's equation two sublattice model of ferrimagnetism, the magnetic moment per formula unit in μ_B, $n_BN(x)$ is expressed as:

$$n_BN(x) = M_B(X) - M_A(X)$$

Where $M_B$and M_A are the B- and A- sublattice magnetic moment in $\mu_B$respectively.

Therefore, increase of calcination temperature for samples the saturation magnetization increases. This may be because increase in the lattice parameter, the exchange interaction between A and B sites gets higher resulting in strengthening of A-B interaction and weakening of B-B interaction , which leads to increase of saturation magnetization. The parameter Ms, Mr and Mr/Ms decrease with increase in Zn concentration [32].

Print ISSN: ISSN 2055-8112(Print); Online ISSN: ISSN 2055-8120(Online)

There is positive relationship between grain size and coercivity (H_c) in the single domain region according to equation: $H_c = g - {}^{h}/_{D^2}$, where g and h are constants and 'D' is the diameter of the particle, this may be because the thermal effects. But the multi domain region there is inverse relationship between grain size and coercivity H_c according to equation: $H_c = a + {}^{b}/_{D}$, where a and b are constants [33, 34, 35,36]. So, the coercivity reduction with increase in Zn concentration & the calcination temperature at 300 °C, 600°C and 900°C, which can be attributed to the reduce in anisotropy field for all Samples , which in turn reduces the domain wall energy for C4 , this refer to results which the Ms ,Mr, Mr/Ms and coercivity values reached.

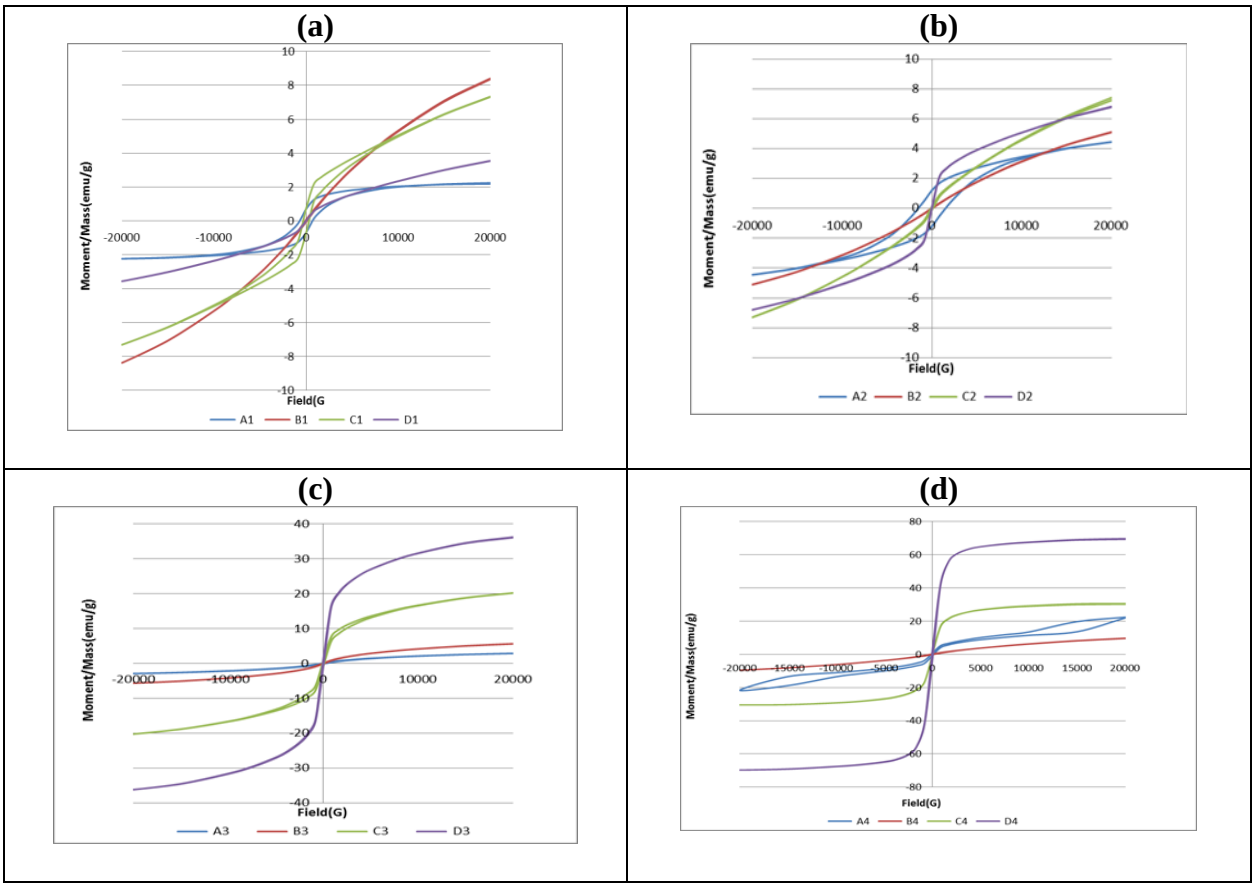

Print ISSN: ISSN 2055-8112(Print); Online ISSN: ISSN 2055-8120(Online)

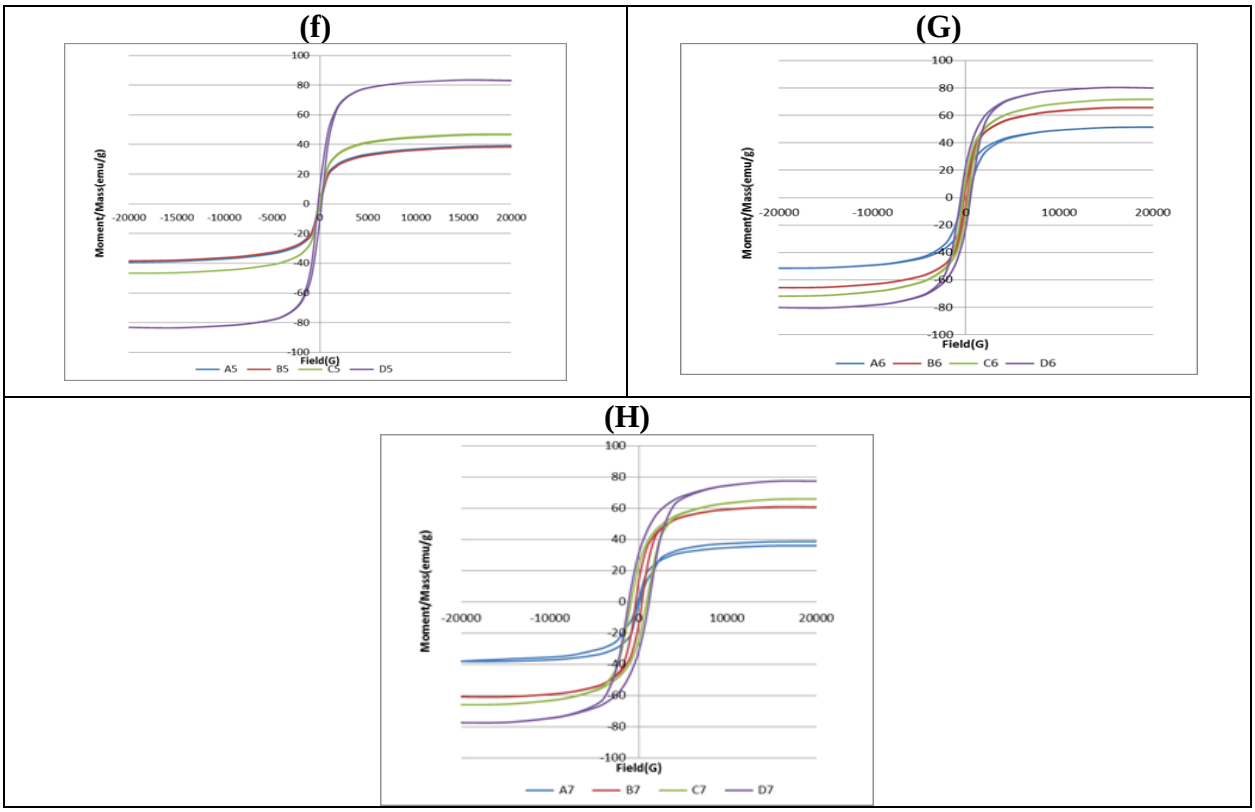

Figure 3.11: the hysteresis loop of the $Co_{1-x}Zn_xFe_2O_4$ nanoparticles at different temperatures.

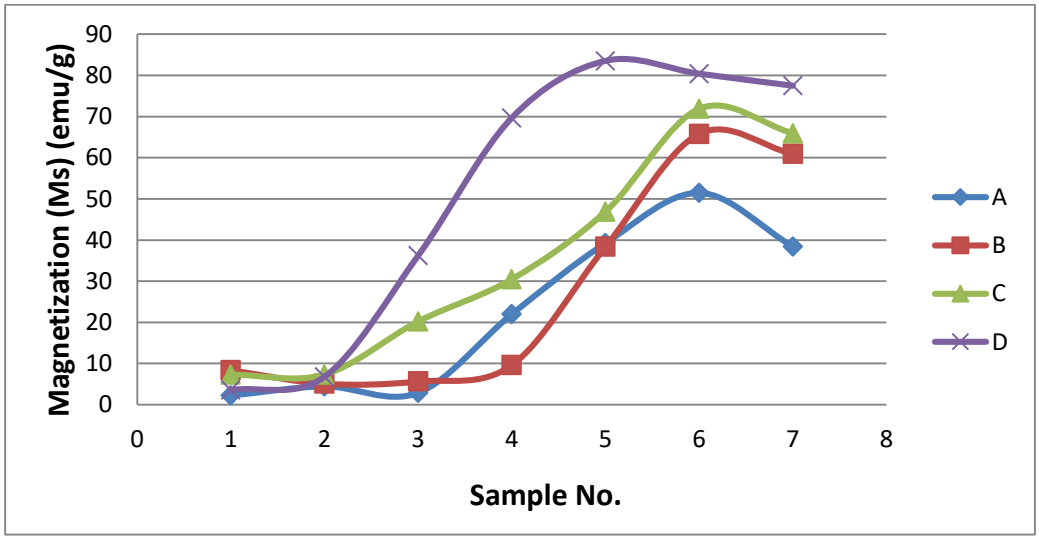

Figure 3.12: The saturation magnetization of the $Co_{1-x}Zn_xFe_2O_4$ nanoparticles at different temperatures

Print ISSN: ISSN 2055-8112(Print); Online ISSN: ISSN 2055-8120(Online)

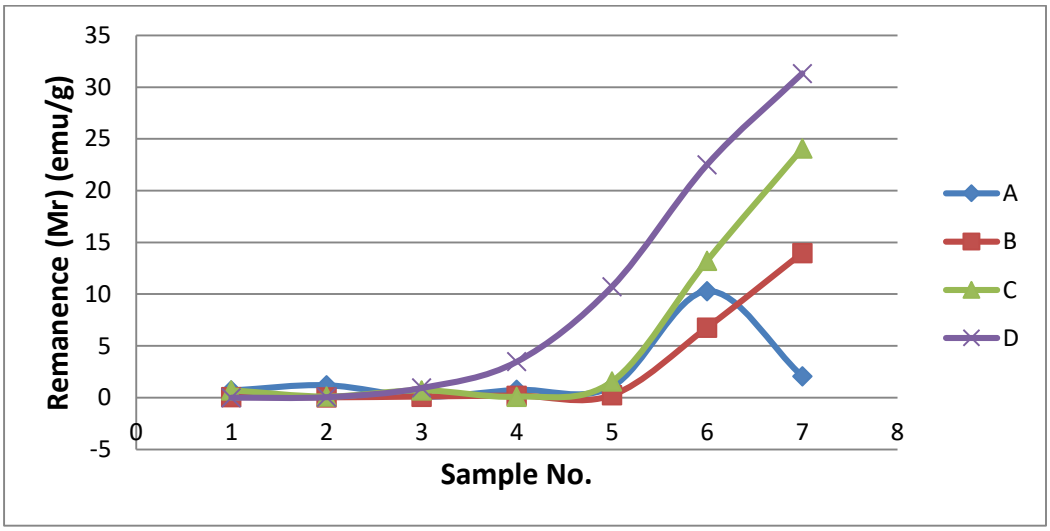

Figure 3.13: The saturation magnetization of the $Co_{1-x}Zn_xFe_2O_4$ nanoparticles at different temperatures

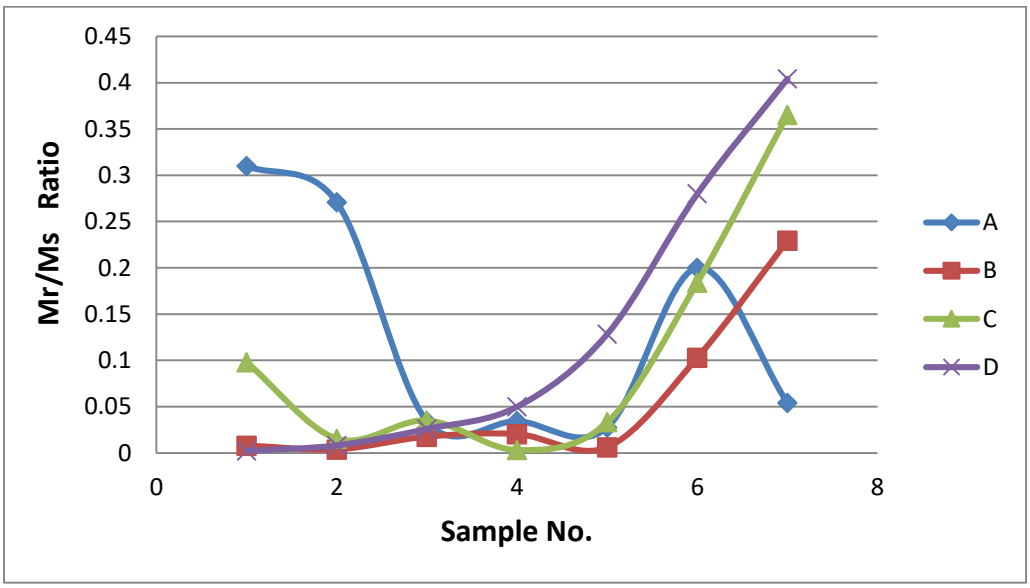

Figure 3.14: The saturation magnetization of the $Co_{1-x}Zn_xFe_2O_4$ nanoparticles at different temperatures

Print ISSN: ISSN 2055-8112(Print); Online ISSN: ISSN 2055-8120(Online)

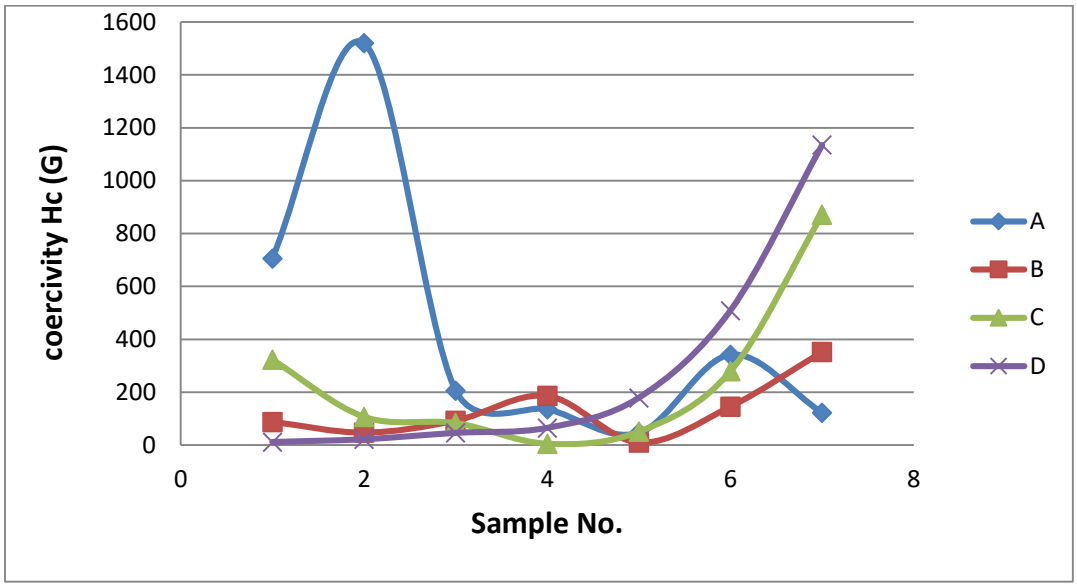

Figure 3.15: The saturation magnetization of the $Co_{1-x}Zn_xFe_2O_4$ nanoparticles at different temperatures.

CONCLUSIONS

The conclusions can be drawn from study of $Co_{1-x}Zn_xFe_2O_4$ nanoparticles at different temperatures fabricated by Co-Precipitation method as following:

1. The crystallite size depend on the Zn concentration & the calcination temperature, where the grain size increase with increasing calcination temperatures from 100 °C to 900°C and its decreased with increasing Zn concentration at 100 ºC, 300 ºC, 600 ºC and inverse trend with 900 ºC.
2. the lattice constant of the $Co_{1-x}Zn_xFe_2O_4$ nanoparticles is increased with increasing calcination temperatures from 100 °C to 900°C and its increased with increasing Zn concentration
3. The crystallinity of $Co_{1-x}Zn_xFe_2O_4$ nanoparticles might be improved by increasing calcination temperature.
4. HRTEM indicates a reliance of particle size and the shape on the Zn concentration & the calcination temperatures. the $Co_{1-x}Zn_xFe_2O_4$ nanoparticles at 100 °C and 300°C has a high degree of agglomeration, but the $Co_{1-x}Zn_xFe_2O_4$ nanoparticles at 600 °C and 900°C has a low degree of agglomeration.
5. The $Co_{1-x}Zn_xFe_2O_4$ nanoparticles at 100 °C, 300°C and 600°C the agglomeration increase with Zn concentration increase, but it's inverse in the $Co_{1-x}Zn_xFe_2O_4$ nanoparticles at 900 °C .

Print ISSN: ISSN 2055-8112(Print); Online ISSN: ISSN 2055-8120(Online)

6. The $Co_{1-x}Zn_xFe_2O_4$ nanoparticles at 100 °C and 300°C take the spherical form with uniform size, but the calcination temperature increase for $Co_{1-x}Zn_xFe_2O_4$ nanoparticles at 600°C occur change in shapes (spherical and Whiskers combination form) with Zn concentration increase but B6 & B7 are spherical form only. The $Co_{1-x}Zn_xFe_2O_4$ nanoparticles at 900°C take the spherical form only with uniform size.
7. EDX analysis of the $Co_{1-x}Zn_xFe_2O_4$ nanoparticles at confirms that the material is composed of Co, Zn, O and Fe without any impurity

8. Hysteresis loop shows a reduction in corecivity with Zn concentration & the calcination temperature for all samples to approximate super-paramagnetic behavior.
9. The C4 ($Co_{0.5}Zn_{0.5}Fe_2O_4$ at 600°C) is best sample in Magnetic &structure properties where it's super-paramagnetic behavior.

10. All laboratory results reveals that the Zn concentration & the calcination temperature play a major role to change its structural and magnetic properties significantly.

REFERENCES

[1] Barbero BP, Gamboa JA, Cadús LE (2006) Synthesis and characterization of La 1-xCaxFeO3 perovskite-type oxide catalysts for total oxidation of volatile organic compounds. Appl Catal B-Environ 65: 21-30.
[2]. Zhao LJ, Zhang HJ, Xing Y, Song SY, Yu SY, et al. (2008) Studies on the magnetism of cobalt ferrite nanocrystals synthesized by hydrothermal method. J Solid State Chem 181: 245-252
[3]. Deraz NM (2008) Production and characterization of pure and doped copper ferrite nanoparticle. J Anal Appl Pyrol 82: 212-222.
[4]. Deraz NM, Shaban S (2009) Optimization of catalytic, surface and magnetic properties of nanocrystalline manganese ferrite. J Anal Appl Pyrol 86: 173-179.
[5]. Ayyappan S, Philip J, Raj B (2009) A facile method to control the size and magnetic properties of CoFe2O4 nanoparticles. Mater Chem Phys115: 712– 717.
[6]. Pradeep A, Priyadharsini P, Chandrasekaran G (2008) Sol–gel route of synthesis of nanoparticles of MgFe2O4 and XRD, FTIR and VSM study. J Magn Magn Mater 320: 2774-2779.
[7]. Li XD, Yang WS, Li F, Evans DG, Duan X (2006) Stoichiometric synthesis of pure NiFe2O4 spinel from layered double hydroxide precursors for use as the anode material in lithium-ion batteries. J Phys Chem Solids 67: 1286- 1290.
[8]. Kale A, Gubbala S, Misra RDK (2004) Magnetic behavior of nanocrystalline nickel ferrite synthesized by the reverse micelle technique. J Magn Magn Mater 277: 350-358.
[9]. Gubbala S, Nathani H, Koizol K, Misra RDK (2004) Magnetic properties of nanocrystalline Ni–Zn, Zn–Mn, and Ni–Mn ferrites synthesized by reverse micelle technique. Physica B 348: 317-328.

[10]. Lee JG, Lee HM, Kim CS (1998) Magnetic properties of CoFe2O4 powders and thin flms

Print ISSN: ISSN 2055-8112(Print); Online ISSN: ISSN 2055-8120(Online)

grown by a sol-gel method. J Magn Magn Mater 177-181: 00-902.
[11]. Davis KJ, Wells S, Upadhyay RV, Charles SW, Grady KO, et al. (1995) The observation of multi-axial anisotropy in ultrafne cobalt ferrite particles used in magnetic fluids. J Magn Magn Mater 149: 14-18.
[12]. Ding J, Mc Cormick PG, Street R (1997) Formation of spinel Mn-ferrite during mechanical alloying. J Magn Magn Mater 171: 309-314.
[13]. Upadhyay RV, Metha RV, Parekh K, Srinivas D, Pant RP (1999) Gdsubstituted ferrite ferrofluid: a possible candidate to enhance pyromagnetic coeffcient. J Magn Magn Mater 201: 129-132.
[14]. Shi Y, Ding J, Liu X, Wang J (1999) NiFe2O4 ultrafne particles prepared by co-precipitation/mechanical alloying. J Magn Magn Mater 205: 249-254.
[15]. Ahmed MA, El-Nimr MK, Tawfk A, Abbo El-Ata AM (1988) Effect of magnetic order on the conductivity in 639-1639-1639-1ferrites. J Mater Sci Lett 7: 639 640.
[16]. Kuanr BK, Srivatava GP (1994) Dispersion observed in electrical properties of titanium-substituted lithium ferrites. J Appl Phys 75: 6115.
[17]. Jeyadevan B, Chinnasamy CN, Shinoda K, Tohji K, Oak H (2003) Mn–Zn ferrite with higher magnetization for temperature sensitive magnetic fluid. J Appl Phys 93: 8450.
[18]. El Sayed AM (2002) Influence of zinc content on some properties of Ni–Zn ferrites. Ceram Int 28: 363-367.

[19]. Ahmed Saied El-Saaey et al, Effect of Zn Substitution on the characterization of Cobalt Ferrite Nano Particles Prepared Co-precipitation method, J Nanomater Mol Nanotechnol 2015, Volume 3 • Issue 4 • 1000155.

[20]. El Sayed AM (2002) Influence of zinc content on some properties of Ni–Znferrites. Ceram Int 28: 363-367

[21] Raeisi Shahraki, et al Structuralcharacterization and magnetic properties of superparamagnetic zinc ferrite nanoparticles synthesized by the coprecipitation method. J. Magn. Magn. Mater. 2012, 324, 3762-3765.

[22] Israf Ud Din et al, Zinc Ferrite Nanoparticle Synthesis and Characterization; Effects of Annealing Temperature on the Size of nanoparticles, Australian Journal of Basic and Applied Sciences, 7(4): 154-162, 2013 ISSN 1991-8178

[23] R. Arulmurugan, B. Jeyadevan, G. Vaidyanathan and S. Sendhilnathan, “Effect of Zinc Substitution on Co-Zn and Mn-Zn Ferrite Nanoferrites Prepared by Co-Precipitation”, J. Magn. Magn. Mater., 288, 2005, 470-477.

[24] Smi, J.; Wijn, H. P. J. Ferrites. Philips Technical Library, Eind-hoven, 1959

[25] Ahmed Saied El-Saaey et al, Effect of Zn Substitution on the characterization of Cobalt Ferrite Nano Particles Prepared Co-precipitation method, J Nanomater Mol Nanotechnol 2015, Volume 3 • Issue 4 • 1000155.

[26] Deraz NM (2010) Glycine-assisted fabrication of nanocrystalline cobalt ferritesystem. J Anal Appl Pyrol 88: 103-109.

Print ISSN: ISSN 2055-8112(Print); Online ISSN: ISSN 2055-8120(Online)

[27]. Deraz NM, Alarif A (2009) Synthesis and characterization of pure and Li2O doped ZnFe2O4 nanoparticles via glycine assisted route. Polyhedron 28: 4122-4130 [17] F. J. Owens and C. P. Poole, The Physics and Chemistry of Nanosolids, New Jersey: John Wiley & Sons, Inc., 2008.

[28] Pradeep A, Chandrasekaran G (2006) FTIR Study of Ni, Cu and Zn Substituted Nanoparticles of MgFe2O4. Material Letters 60: 371-374.
[29] Koseoglu Y, Bay M, Tan M, Baykal A, Sozeri H, et al. (2010) Magnetic and dielectric properties of Mn0.2Ni0.8Fe2O4 nanoparticles synthesized by PEGassisted hydrothermal method. J Nanopart Res 13 (2010) 2235-2244.

[30] Waldron RDD (1955) Infrared Spectra of Ferrite. Physical Review 99: 1727- 1735.

[31] A. Gaber etal ,Influence of Calcination Temperature on the Structure and Porosity of Nanocrystalline SnO2 Synthesized by a Conventional Precipitation method, Int. J. Electrochem. Sci., 9 (2014) 81 – 95.

[32]S. Nasrin et al , Influence of Zn substitution on the structural and magnetic properties of Co1-xZnxFe2O4 nano-ferrites, (IOSR-JAP),e- 2278-4861.Volume 6, Issue 2 Ver. III (Mar-Apr. 2014), PP 58-65.

[33] B. D. Cullity, "Introduction to Magnetic Materials," AddisonWesely Publishing Company Inc., Reading, Massachusetts,1972.
[34] Berkowitz AE, Schuele WJ (1959) Magnetic properties of some ferrite micropowders. Journal of Applied Physics 30: S134-S134.

[35] M. George, A. M. John, S. S. Nair, P. A. Joy and M. R. Anantharaman, "Finite Size Effects on the Structural and Magnetic Properties of Sol-Gel Synthesized NiFe2O4 Powders," Journal of Magnetism and Magnetic Materials,Vol. 302, No. 1, 2006, pp. 190-195.

[36] He HY (2011) Comparison study on magnetic property of Co0.5Zn0.5Fe2O4 powders by template-assisted sol–gel and hydrothermal methods. J Mat Sci: Mater Electron 23: 995-1000.

Print ISSN: ISSN 2055-8112(Print); Online ISSN: ISSN 2055-8120(Online)